Fabrication and characterization of Ti6Al4V by selective electron beam and laser hybrid melting

Bin Zhou[1,2,3], Jun Zhou[1,2,3], Hongxin Li[1,2,3], Feng Lin[1,2,3,*]

[1]Department of Mechanical Engineering, Tsinghua University, Beijing 100084, China

[2]Biomanufacturing and Rapid Forming Technology Key Laboratory of Beijing, China

[3]Key Laboratory for Advanced Materials Processing Technology, Ministry of Education of China

Abstract

A hybrid process, which combines electron beam selective melting(EBSM) and selective laser melting(SLM), is proposed in this study. Laser is led into the vacuum chamber through the lens so that laser can be used to fabricate the metal powder at the same time with electron beam. In this study, Laser is used to pre-preheat the metal powder in order to preventing powder spreading and laser is also used to fabricate the contour of the parts both inside and outside. Electron beam is used to preheat the metal powder to the specified temperature and to fabricate the interior of the parts. It can be sure that through the hybrid process we can fabricate the parts with both better surface quality, higher precision and higher efficiency. Ti6Al4V samples were fabricated by selective electron beam and laser hybrid melting. The surface roughness of the parts was measured, the microstructures of the contour and interior were characterized using scanning electron microscopy (SEM). The results are that as-fabricated parts have better surface quality than the parts fabricated only using EBM process.

Keywords: Electron beam selective melting; Selective laser melting; Hybrid; Ti6Al4V

Introduction

Selective laser melting (SLM) and electron beam selective melting (EBSM) are powder-based additive manufacturing technology, which utilize a focused electron beam/laser beam to melt and fuse metal powder by rapid self-cooling, and produce parts layer by layer with high accuracy. So that both SLM and EBSM can be applied in impeller, blade, porous structure and medical implants manufacturing [1-2]. SLM process is with higher precision and better surface roughness, because laser spot diameter, layer thickness and powder diameter are smaller. But the material absorption rate of laser is low, so the powder layer of SLM is thin (20μm - 50μm), which led to the forming efficiency of SLM is low (about 20cm^3/ h). EBSM has many unique characteristics such as high energy efficiency, high scan speed, and moderate operation cost. The material absorption rate for the electron beam is much higher(about 80%), the powder bed temperature of EBSM is much higher (about 600℃-1000℃)[3-5]. So EBSM process has a high forming efficiency (which can be up to 80cm3 / h). But the precision and surface roughness of EBSM is worse than that of SLM. The surface roughness of the EBM parts spread over a broad range but could often exceeds 30μm depending on various factors such as process parameters, material types, powder characteristics and surface orientations [6-9].

It is difficult to obtain high precision and efficiency at the same time with single forming process. Jose Coronel [10] proposed a Multi-3D System which combines CNC router in additive manufacturing process, aimed to increase the accuracy of the printing parts. This process will reduce the forming efficiency and cause material waste. Li Yang [11] investigated the feasibility of utilizing electro polishing for the direct treatment of Ti6Al4V parts fabricated by EBM. This is the post-process and will cost material lost and distortion. H. Schleifenbaum [12-16] developed a new prototype machine tool including a kW laser and a multi-beam system. The core of the parts can be fast manufactured with a large beam diameter while the skin is manufactured with a small beam diameter in order to assure the part`s accuracy and detail resolution. But high power laser beam causes serious powder spattering which has a negative effect in the process as a whole.

In this study, a hybrid process was proposed, which combined electron beam selective melting(EBSM) and selective laser melting(SLM). The advantages of both EBSM and SLM can be obtained in the hybrid process with high precision and efficiency at the same time. Ti6Al4V samples were fabricated by the hybrid process. The surface roughness of the samples was measured, the microstructures of the contour and interior were characterized using scanning electron microscopy (SEM).

Selective electron beam and laser hybrid melting process

Electron beam selective melting(EBSM) process and selective laser melting(SLM) process are combined into a hybrid melting process. In the hybrid melting process, both the electron beam and laser can preheat and fabricate the powder at the same time or at interval. It shares one powder supply process and powder spread process and the whole system is in one vacuum chamber.

Laser is used to fabricate the contour of the parts both inside and outside. Thus samples are fabricated with high precision and good surface roughness. Electron beam is used to fabricate the interior of the parts with high scanning speed, which can increase the forming efficiency (as shown in Fig. 1).

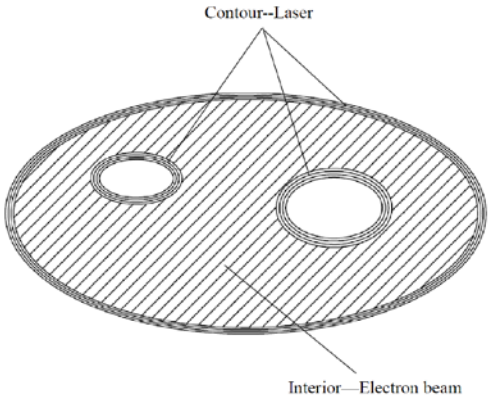

Fig. 1 EB and laser scanning section

In the hybrid melting process, steps are shown in Fig. 2. First of all, electron beam is used to preheat the powder bed to the specified temperature; then, powder is supplied and spread; Next, laser is used to pre-preheat the metal powder in order to preventing powder spreading; and after that, electron beam is used to preheat the powder bed to the specified temperature; Subsequently, electron beam is used to fabricate the interior of the parts and laser is used to fabricate the contour of the parts.

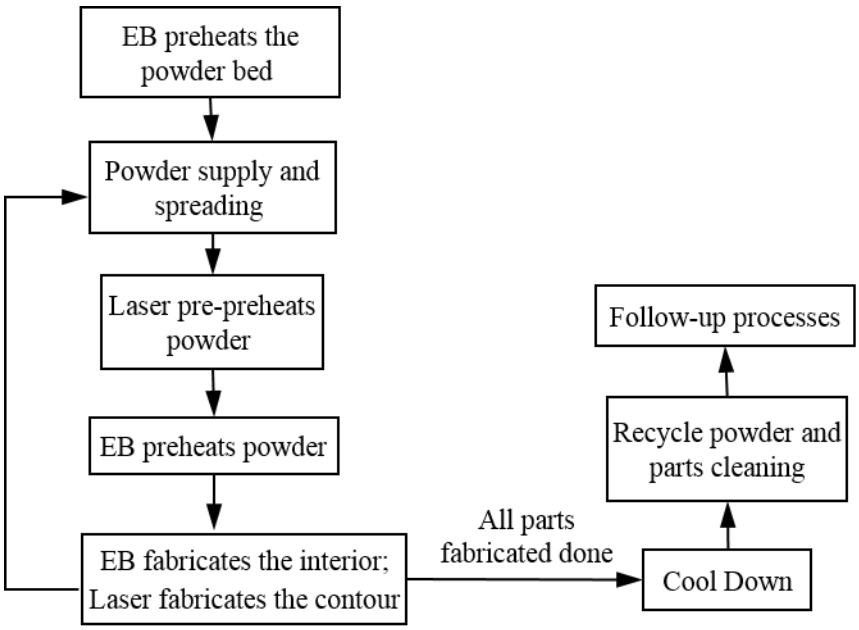

Fig. 2 Hybrid process flow diagram

Development of hybrid equipment

On the basis of self-designed EBSM-250 electron beam selective melting system by Tsinghua University, laser was led to vacuum chamber through the lens of chamber wall, with dynamic focusing scanning system outside vacuum chamber (as shown in Fig. 3).

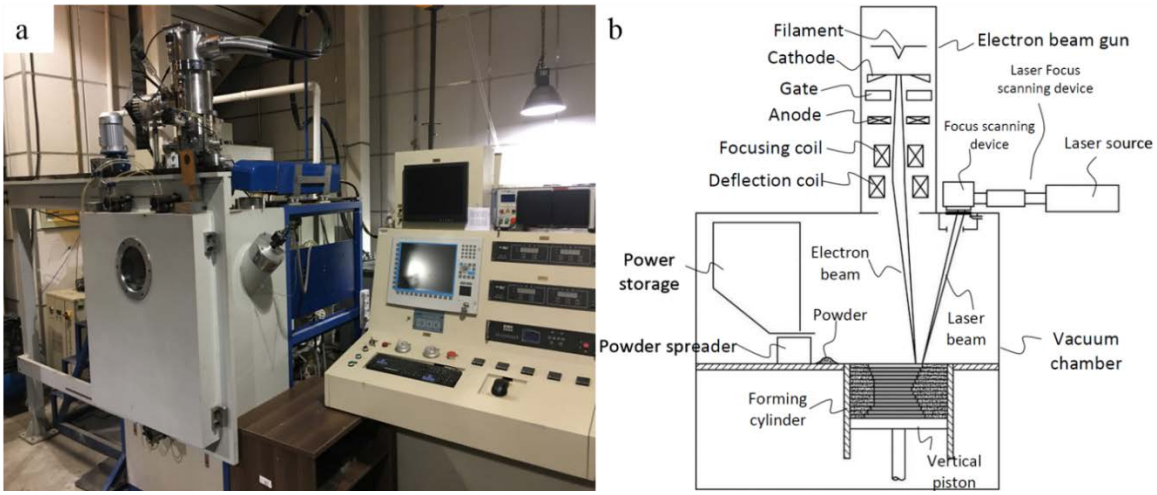

Fig. 3 (a) Hybrid forming system; (b) Schematic diagram of system

The hybrid equipment characteristics are shown in Table 1. The maximum power of the electron beam is 3kW, and YLR-200 ytterbium fiber laser has maximum power of 200 W (IPG Laser GmbH, Germany).

Table 1 The hybrid equipment characteristics

	Electron beam	Laser
Effective build volume [mm×mm×mm]	200×200×200	
Power [W]	3000	200
Scanning speed [mm/s]	0 ~ 20000	0 ~ 2000
Beam diameter [μm]	200 ~ 400	100 ~ 200
Pressure [Pa]	1×10^{0} ~ 1×10^{-3}	
Powder bed temperature [℃]	20 ~ 1000	

Since both the electron beam and laser scanning focusing system has their own coordinate systems, it is necessary to unified these two coordinate systems into the substrate coordinate system. Laser scanning head is placed on the top of the vacuum chamber next to the electron gun and has an angle (β=8°) rotation around the Y-axis direction. Also, the center of the laser scanning head has a distance with the center of electron gun (as shown in Fig. 4). Coordinate translation and rotation transformation is needed.

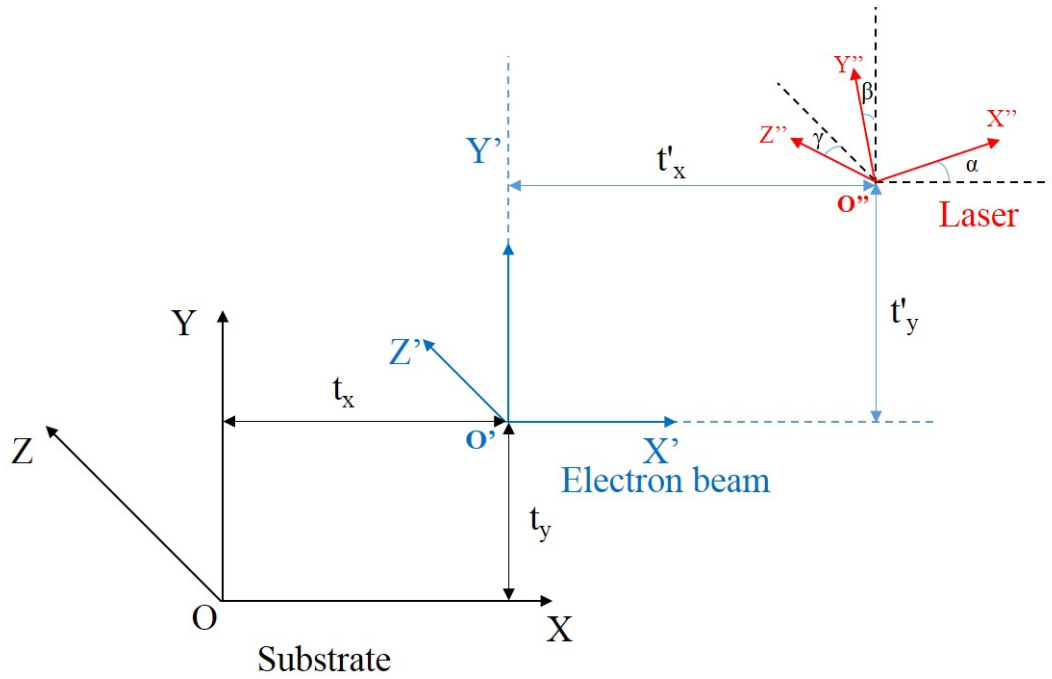

Fig. 4 Three coordinate systems

Relative to the substrate coordinate system, the electron beam coordinate system has just translation transformation. But as to the laser coordinate system, it has both translation and rotation

transformation.

$$\begin{pmatrix} x' & y' & z' & 1 \end{pmatrix} = \begin{pmatrix} x & y & z & 1 \end{pmatrix} \begin{bmatrix} 1 & 0 & 0 & 0 \\ 0 & 1 & 0 & 0 \\ 0 & 0 & 1 & 0 \\ t_x & t_y & t_z & 1 \end{bmatrix} \quad \text{..... (1)}$$

From the translation transformation of formula (1), since t_z=0, we can get:

$$\begin{cases} x' = x + t_x \\ y' = y + t_y \\ z' = z \end{cases} \quad \text{..... (2)}$$

As to the laser coordinate system, two steps are needed. First is translation transformation and second is rotation transformation.

$$\begin{pmatrix} x'' & y'' & z'' & 1 \end{pmatrix} = \begin{pmatrix} x & y & z & 1 \end{pmatrix} \begin{bmatrix} 1 & 0 & 0 & 0 \\ 0 & 1 & 0 & 0 \\ 0 & 0 & 1 & 0 \\ t_x + t'_x & t_y + t'_y & t_z + t'_z & 1 \end{bmatrix} \begin{bmatrix} 1 & 0 & 0 & 0 \\ 0 & \cos\alpha & \sin\alpha & 0 \\ 0 & -\sin\alpha & \cos\alpha & 0 \\ 0 & 0 & 0 & 1 \end{bmatrix} \begin{bmatrix} \cos\beta & 0 & -\sin\beta & 0 \\ 0 & 1 & 0 & 0 \\ \sin\beta & 0 & \cos\beta & 0 \\ 0 & 0 & 0 & 1 \end{bmatrix} \begin{bmatrix} \cos\gamma & \sin\gamma & 0 & 0 \\ -\sin\gamma & \cos\gamma & 0 & 0 \\ 0 & 0 & 1 & 0 \\ 0 & 0 & 0 & 1 \end{bmatrix}$$

..... (3)

From the translation and rotation transformation of formula (3), since α=γ=0°, we can get:

$$\begin{cases} x'' = \left(z + t_y + t'_y\right) \cdot \sin\beta + \left(x + t_x + t'_x\right) \cdot \cos\beta \\ y'' = y + t_y + t'_y \\ z'' = \left(z + t_y + t'_y\right) \cdot \cos\beta - \left(x + t_x + t'_x\right) \cdot \sin\beta \end{cases} \quad \text{..... (4)}$$

For any point in the CAD file, it can be transformed into both the electron beam and laser controller by formula (3) and formula (4).

In the hybrid melting process, since the forming process is carried out under vacuum, the evaporation of volatile material such as Al is much greater and the lenses will be steamed with metal vapor. After a long time working, the laser power will be absorbed by the lens and eventually the lens will be broken. As a result, the hybrid process is seriously affected.

Anti-evaporation system was designed to prevent the lenses (as shown in Fig. 5). In front of the lens, a second lens was placed, which was bigger than the behind one. The second lens could rotate round the axis. The laser working area which laser passes through to the substrate, was in one side and the brush was in the other side. As-designed system could allow lens working with cleaning at the same time and the brush would not disturb the process.

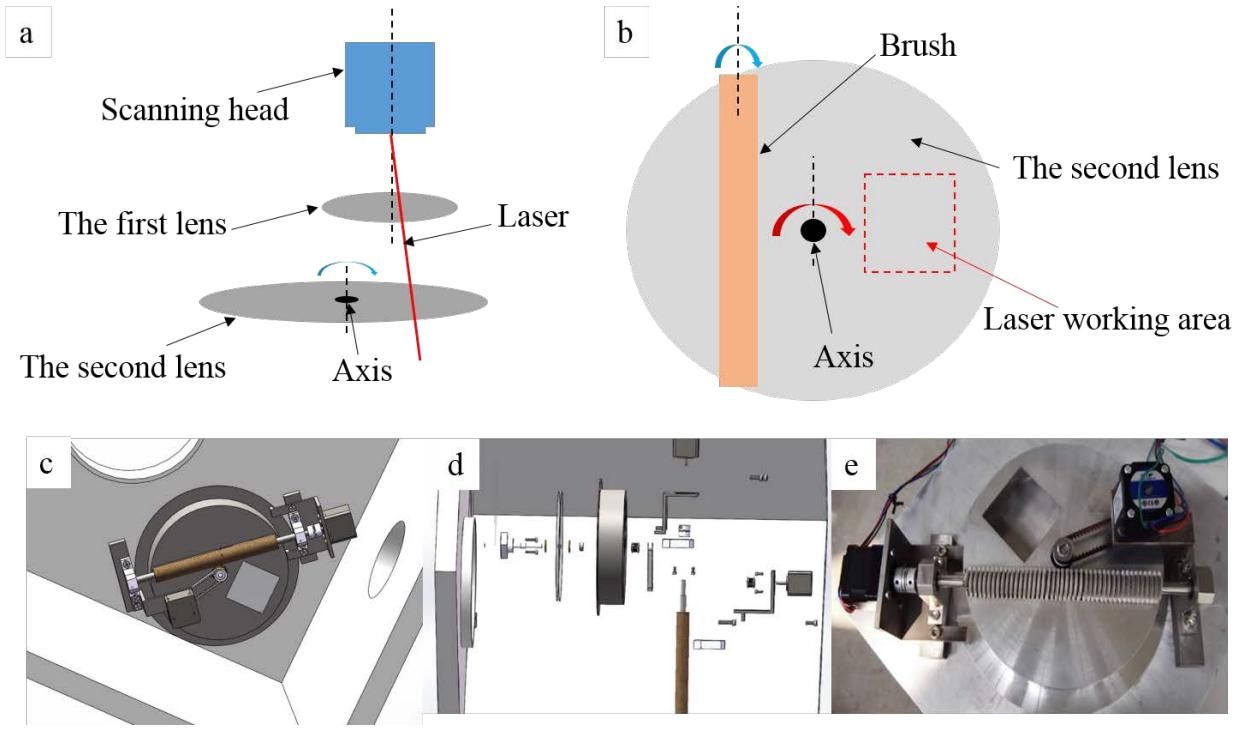

Fig. 5 Anti-evaporation system

Hybrid melting experiment

Atomized spherical Ti6Al4V powder (shown in Fig. 6) were used in hybrid melting process. The powder particle size was in the range of 13~55μm, with an average of 32μm, which is obtained by laser particle size analyzer Hydro 2000MU (A). The powder size distribution is shown in Fig. 7 and the composition is shown in Table 2.

Table 2 Ti6Al4V powder composition

Element	Ti	Al	V	C	N	O
wt%	Balance	6.05	3.94	0.02	0.02	0.087

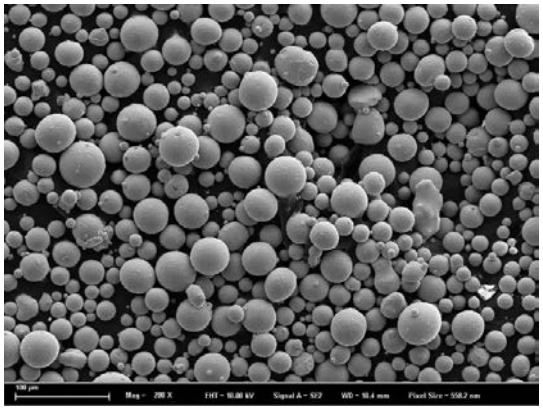

Fig. 6 SEM image of Ti6Al4V powders

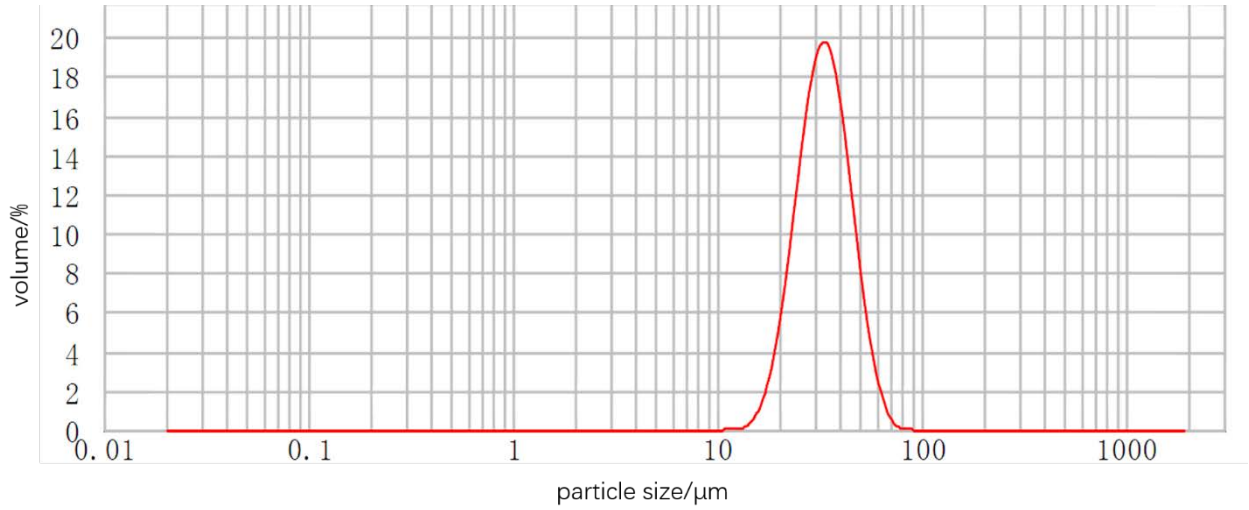

Fig. 7 Ti6Al4V powder size distribution

Three Ti6Al4V samples were fabricated with the electron beam and laser (as shown in Fig. 8). The size of the samples were 20mm×20mm. The hybrid process was shown in Fig. 8(b), which used laser scanning the contour and EB scanning interior of the sample. To be comparison, two samples were fabricated which respectively used laser (Fig. 8(a)) and EB (Fig. 8(c)) scanning both the contour and interior. The powder layer thickness is 0.03mm, and 100 layers were fabricated for each three samples. The laser power was 100W, with scanning speed 200 mm/s and hatching space 0.05mm. As for EB, the power is 180W, and scanning speed is 250 mm/s with hatching space 0.1mm. The pressure was 2×10^{-3}Pa, and the substrate was made of Ti6Al4V with thickness of 10mm. The powder bed temperature is controlled to 700-800℃ (as shown in Table 3).

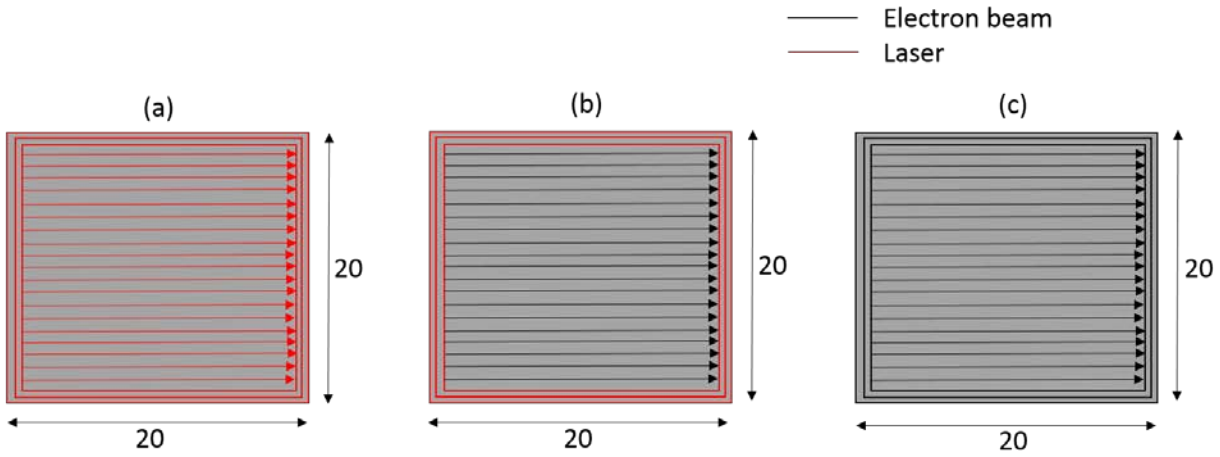

Fig. 8 (a) Laser scanning contour and interior; (b) Laser scanning contour and EB scanning interior; (c) EB scanning contour and interior;

Table 3 Ti6Al4V fabrication parameters

	Electron beam	Laser
Power [W]	180	100
Scanning speed [mm/s]	250	200
Hatching space [mm]	0.1	0.05
Layer thickness [mm]	0.03	
Pressure [Pa]	2×10^{-3}	
Powder bed temperature [℃]	700 ~ 800	

The morphologies and microstructure of the Ti6Al4V samples were analyzed using a scanning electron microscope. The defect and pore were measured through the analysis of SEM images. The samples surfaces of samples were etched with Kroll's reagent: 1% HNO3, 2% HF and 97% of distilled water. The density of the Ti6Al4V parts were measured by the method of drainage, using digital machine (ADVENTURER, AR423DCN) with an accuracy of 0.001 g. The surface roughness was measured by Surface topography measuring instrument (TalySurf Intra, Britain).

The surface roughness results are shown in Table 4. The surface roughness of the side is mainly influenced by electron beam or laser parameters, powder size, layer thickness and powder bed temperature. In this study, three samples were fabricated in the same condition which shared the same powder size, layer thickness and powder bed temperature. So the differences of the side surface roughness of the samples result in the differences of the power parameters. From the measurement results, the side surface roughness of the samples with laser scanning contour and EB scanning interior (11.53μm) is better than the samples with EB scanning contour and interior (17.30μm) and a little worse than the samples with laser scanning contour and interior (9.75μm). Because the laser beam spot is smaller (100-200μm) than the electron beam (200-400μm), the side surface roughness of the samples fabricated by hybrid melting process increases. And because of the higher absorption rate of electron beam, temperature of the molten pool of the hybrid melting fabricated samples is higher than that of laser fabricated one. This may cause the side surface roughness a little worse. As to the top, the surface roughness is mainly influenced by electron beam or laser parameters. The input energy density is higher; the surface roughness is better. Because of the high absorption rate of electron beam, the input energy density of electron beam is much higher than laser. As a result, the top surface roughness of EB is better than that of laser. Almost of the top areas of hybrid melting fabricated samples are scanned by electron beam, so the top surface roughness is almost the same with electron beam fabricated one.

Table 4 Ti6Al4V surface roughness

Surface roughness R_a[μm]	(a) Laser scanning contour and interior	(b) Laser scanning contour and EB scanning interior	(c) EB scanning contour and interior
Top	14.70	2.28	3.14
Side	9.75	11.53	17.30

The microstructures of hybrid melting fabricated Ti6Al4V are shown in Fig. 9. The interior fabricated by electron beam is dense with almost no pores and defects (Fig. 9a and Fig. 9c). While, the contour fabricated by laser has many visible pores and defects (Fig. 9a and Fig. 9b). The laser power in not enough to melt the powder densely, which is needed to be increased. In the hybrid melting process, powder is fabricated layer by layer. The molten pool has high temperature and fast cooling speed, and the solidified part is repeatedly heated and cooled, which results in the formation and transformation of organization with the forming process. When metal molten pool solidifies, the temperature gradient along the building direction is much larger than the other direction, So the crystal grains grow in columnar crystal βphase along the building direction. Subsequently, with the rapid cooling of molten pool, β phase is transformed into metastable fine acicular martensite without diffusion. Then because of the effect of reheating, metastable fine acicular martensite breaks down, forming elongated and coarse lamellar α+βphase. The final microstructure is mainly composed of fine acicular martensite, elongated lamellar αphase and coarse lamellar αphase. Due to the material absorption rate of electron beam is much higher than that of laser, and the molten pool temperature is higher, so in the microstructure of electron beam fabricated Ti6Al4V, αphase is much coarser in the basket-weave microstructure (Fig. 9d-e).

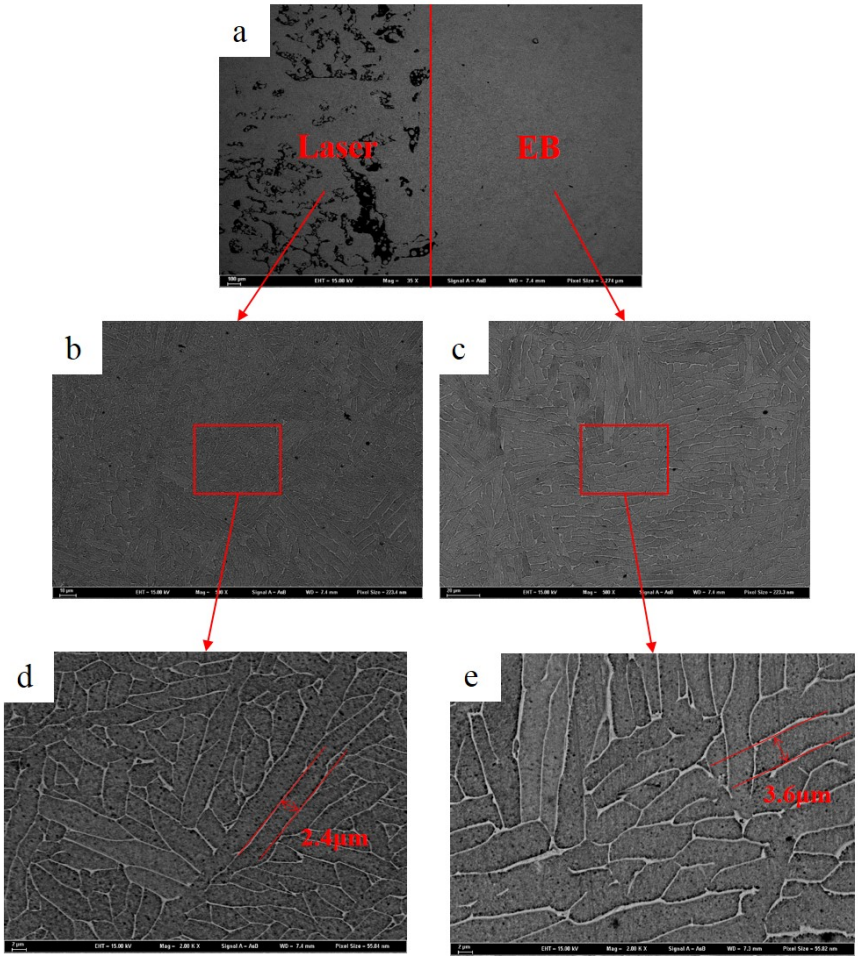

Fig. 9 SEM images of hybrid melting fabricated Ti6Al4V

Conclusions

The electron beam and laser hybrid melting process was proposed and the hybrid forming equipment was developed. Ti6Al4V samples fabricated by electron beam and laser hybrid melting process, which used laser scanning the contour and electron beam scanning the interior, have better surface roughness than electron beam fabricated samples. And the hybrid process has a much higher forming efficiency than SLM process or EBSM process with post-treatments.

Acknowledgement

This work was supported by 'Suzhou-Tsinghua special innovation leading action' program.

References

[1]. Ge Wenjun, Guo Chao, Lin Feng, Microstructures of Components Synthesized via Electron Beam Selective Melting Using Blended Pre-Alloyed Powders of Ti6Al4V and Ti45Al7Nb, Rare Metal Materials and Engineering, 44 (2015): 2623-2627

[2]. Dylan Agius, Kyriakos I. Kourousis, Chris Wallbrink, Tingting Song, Cyclic plasticity and microstructure of as-built SLM Ti-6Al-4V: The effect of build orientation, Materials Science and Engineering: A, 701(2017): 85-100

[3]. Xiaoli Zhao, Shujun Li, Man Zhang, Yandong Liu, Timothy B. Sercombe, Shaogang Wang, Yulin Hao, Rui Yang, Lawrence E. Murr, Comparison of the microstructures and mechanical properties of Ti–6Al–4V fabricated by selective laser melting and electron beam melting, Materials & Design, 95(2016):21-31

[4]. J.P. Kruth, L. Froyen, J. Van Vaerenbergh, P. Mercelis, M. Rombouts, B. Lauwers, Selective laser melting of iron-based powder, Journal of Materials Processing Technology, 149(2004):616-622

[5]. I. Yadroitsev, Ph. Bertrand, I. Smurov, Parametric analysis of the selective laser melting process, Applied Surface Science, 253(2007): 8064-8069

[6]. Denis Cormier, Ola Harrysson, Harvey West, Characterization of H13 steel produced via electron beam melting, Rapid Prototyping Journal, 10 (2004):35-41

[7]. Zäh, M.F. & Lutzmann, S. Modelling and simulation of electron beam melting. Production Engineering. 4(2010): 15-23.

[8]. Xibing Gong, Ted Anderson, Kevin Chou. Review on powder-based electron beam additive manufacturing technology. Manufacturing Review 1 (2014): 2

[9]. Xipeng Tan, Yihong Kok, Yu Jun Tan, Guglielmo Vastola, Qing Xiang Pei, Gang Zhang, Yong-Wei Zhang, Shu Beng Tor, Kah Fai Leong, Chee Kai Chua. An experimental and simulation study on build thickness dependent microstructure for electron beam melted Ti–6Al–4V, Journal of Alloys and Compounds, 646(2015);303-309

[10]. Coronel, Jose Luis, Jr. Multi3D system: Advanced manufacturing through the implementation of material handling robotics. The University of Texas at El Paso, USA, 2015

[11]. L. Yang, Yan Wu, A. Lassell, Bin Zhou. Electropolishing of Ti6Al4V Parts Fabricated by

Electron Beam Melting. Proceedings of Solid Freeform Fabrication (SFF) Symposium, Austin, TX, 2016.

[12]. H. Schleifenbaum, W. Meiners, K. Wissenbach, C. Hinke, Individualized production by means of high power Selective Laser Melting, CIRP Journal of Manufacturing Science and Technology, 2(2010):161-169

[13]. D. Buchbinder, H. Schleifenbaum, S. Heidrich, W. Meiners, J. Bültmann, High Power Selective Laser Melting (HP SLM) of Aluminum Parts, Physics Procedia, 12(2011): 271-278

[14]. Bremen, S., Schrage, J., Meiners, W., Wissenbach, K., High power Selective Laser Melting - further steps towards series production, Proceedings of the International Conference on Additive Manufacturing, 9-10 July, 2012, Loughborough, UK, 19 S. (2012)

[15]. HO_slm_optical_systems_for_high_power slm_2012.pdf，http://www.ilt.fraunhofer.de/

[16]. HO_slm_high_power_slm-machining_of_inconel_718_2012.pdf，

http://www.ilt.fraunhofer.de/